

A nanoscale Ti/GaAs metal-semiconductor hybrid sensor for room temperature light detection

A. K. M. Newaz,^{1,a)} W.-J. Chang,² K. D. Wallace,³ L. C. Edge,¹ S. A. Wickline,³ R. Bashir,^{2,4} A. M. Gilbertson,⁵ L. F. Cohen,⁵ and S. A. Solin^{1,5,b)}

¹Department of Physics, Center for Material Innovations, Washington University in St. Louis, St. Louis, Missouri 63132, USA

²Micro and Nanotechnology Laboratory, University of Illinois at Urbana-Champaign, Urbana, Illinois 61801, USA

³Department of Medicine, Washington University in St. Louis, St. Louis, Missouri 63132, USA

⁴Department of Electrical and Computer Engineering and Bioengineering, University of Illinois at Urbana-Champaign, Urbana, Illinois 61801, USA

⁵Blackett Laboratory, Imperial College, London SW7 2BZ, United Kingdom

(Received 22 June 2010; accepted 17 July 2010; published online 24 August 2010)

We report an individually addressable Ti/GaAs metal-semiconductor hybrid optical nanosensor with positive photoresistance and a sensitivity that *increases* as the device dimensions shrink. The underlying physics relates to the crossover from ballistic to diffusive transport of the photoinduced carriers and the geometric enhancement of the effect associated with a Schottky-barrier-coupled parallel metal shunt layer. For a 250 nm device under 633 nm illumination we observe a specific detectivity of $D^* = 5.06 \times 10^{11}$ cm $\sqrt{\text{Hz/W}}$ with a dynamic response of 40 dB. © 2010 American Institute of Physics. [doi:10.1063/1.3480611]

The ongoing effort to develop inexpensive optical sensors with high sensitivity and reduced size in the submicron regime is driven by the positive impact they would have on a number of disciplines ranging from medical instrumentation to consumer electronics.¹ While much progress has been made² and sensors as small as 100 nm have been reported,³ structures with dimensions below 500 nm are typically incompatible with the fabrication methods that stimulate commercialization. In this letter, we describe an individually addressable 250 nm positive photoresistance optical sensor that exhibits significant room temperature sensitivity in the visible spectral region and can be fabricated using conventional methods. Positive photoresistance (negative photoconductivity) has been observed in macroscopic semiconductor heterostructures⁴ and nanoparticle films.⁵ However, the nanoscale Ti/GaAs metal/semiconductor hybrid structures (MSHs) we describe here function via a fundamentally distinct principle; the photoinduced switching from ballistic⁶ to diffusive transport of carriers. This results in a scale-dependent positive photoresistance (SDPP) that *increases with decreasing* dimensions. The photoresistive effect in an MSH, results from photocarrier-induced electrical current reallocation between the semiconductor and metal that changes the effective resistance.

The MSH structures we study, consist of a Au/Ti top surface layer that makes a Schottky contact to the underlying GaAs. We refer hereafter to the Au/Ti layer as the shunt (see below.) The details of the structure are shown in Fig. 1. Our devices were prepared on lattice-matched 90 nm thick Si-doped GaAs epitaxial layers ($\mu = 3225$ cm² V⁻¹ S⁻¹, $N_D = 4 \times 10^{17}$ cm⁻³)⁷ grown by molecular beam epitaxy. All MSH we prepared had a fixed geometrical arrangement of the mesa, shunt, and metal leads but varied in scale/size from

macroscopic (5 μm , 1 μm) to nanoscopic (500 nm, 250 nm) as shown for the largest and smallest devices in the scanning electron micrographs of Fig. 2. To directly ascertain the effect of the shunt, equivalent but shuntless reference devices were also studied. A minimum of four devices for each device size has been studied; all devices of a specific size show equivalent results. Details of the device fabrication procedures are described elsewhere.⁸

All optical and transport measurements presented here were carried out at room temperature. Our devices employ a modified van der Pauw mesa structure in which current is applied between leads 1 and 2 and voltage is measured between leads 3 and 4 [see Fig. 2(a)]. The four-point resistance is defined as $R = V_{34}/I_{12}$. The spatial sensitivity of the SDPP devices has been measured by recording the lateral positional dependence of R (image plot) as an unfocused He-Ne laser beam (TEM₀₀ mode, beam waist diameter 800 μm , output 5 mW, and wavelength 632.8 nm) traverses the sensor area in steps, down to 10 μm .

The Ti/GaAs interface forms a well-characterized Schottky barrier while the Au/Ti layer acts as a shunt for current crossing the barrier (hence, the name).⁸ Thus, in contrast to typical top-gated structures such as FETs, the shunt provides an important and intended current path. Moreover,

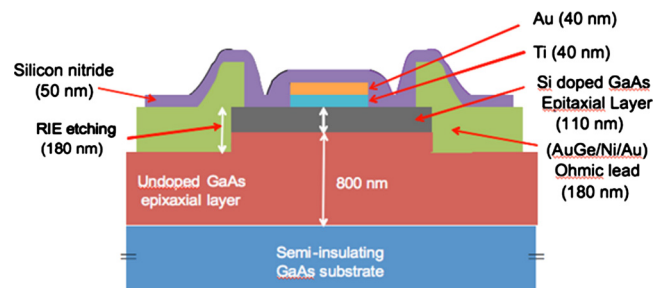


FIG. 1. (Color online) A cross-sectional view of the structure of the SDPP device.

^{a)}Present address: Department of Physics and Astronomy, Vanderbilt University, Nashville, TN 37235, USA.

^{b)}Electronic mail: solin@wuphys.wustl.edu.

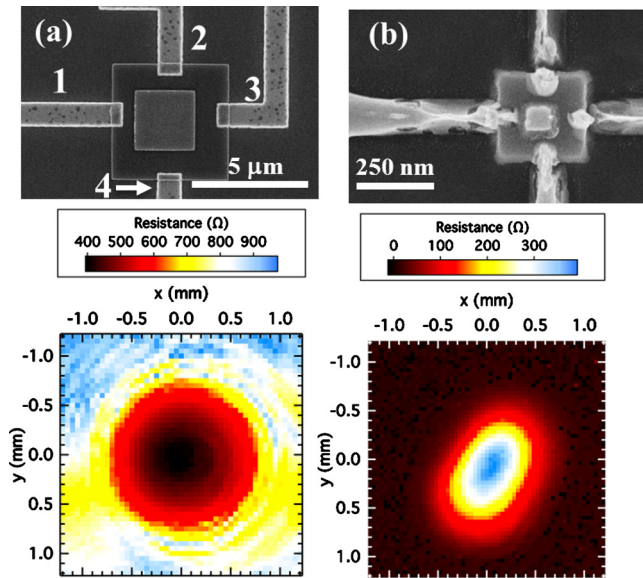


FIG. 2. (Color online) SEM images (top panel) and resistance image plots (bottom panel) of the $5\ \mu\text{m}$ device (a) and $250\ \text{nm}$ device (b). Panel (a) shows the contact labeling scheme. All image plots were acquired with an ac bias of peak current $I_{34}=100\ \text{nA}$.

even though the shunt is essentially opaque at $633\ \text{nm}$, illumination of the exposed GaAs mesa at that wavelength is sufficient to promote current flow through it as demonstrated by the direct I-V measurements shown in Fig. 3. The I-V characteristic changes from Schottky-like to Ohmic at high illumination. This is accompanied by a reduction in the zero bias resistance by a factor of 209 with an illumination intensity change of $10^{-5} I_0$ to I_0 , where I_0 is $1\ \text{W}/\text{cm}^2$. The intensity-dependent open circuit voltage seen in Fig. 3 is characteristic of illuminated Schottky barriers⁹ and in our case is no doubt caused by the migration of photogenerated carriers into the interface/depletion region.

A two-dimensional image plot for the $5\ \mu\text{m}$ device is shown in Fig. 2(a). The general features observed for the image plot of the $1\ \mu\text{m}$ device are similar. The resistances of these devices are large when the laser spot is far from the device center (minimum illumination intensity) and smallest when the laser is approximately centered on the device (maximum illumination intensity). If we define the relative photoresistance as $\delta R(P, \lambda) = [R(P) - R_0] / R_0 \times 100\%$, where R_0 is the dark resistance, P is the total power illumi-

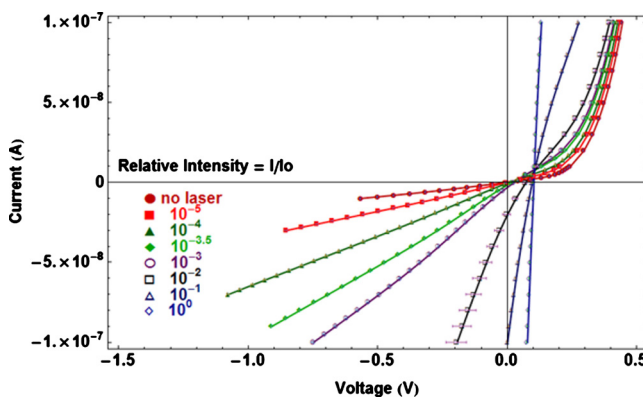


FIG. 3. (Color online) The intensity dependence of the two-point I-V characteristic of the Schottky diode component of a $5\ \mu\text{m}$ SDPP device ($I_0=1\ \text{W}/\text{cm}^2$).

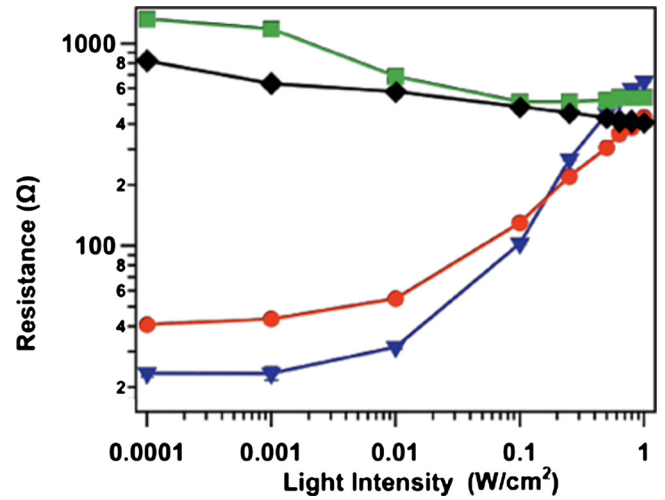


FIG. 4. (Color online) The dynamic responses of SDPP devices of different sizes to illumination by $632.8\ \text{nm}$ radiation. Device size: \blacklozenge — $5\ \mu\text{m}$, \blacksquare — $1\ \mu\text{m}$, \bullet — $500\ \text{nm}$, and \blacktriangledown — $250\ \text{nm}$.

inating the active region, and λ is the wavelength then the maximum $\delta R(P, \lambda)$ values for the $5\ \mu\text{m}$ ($R_0=978\ \Omega$) and $1\ \mu\text{m}$ ($R_0=1301\ \Omega$) devices are both 58% for maximum illumination of $P=100\ \text{nW}$ and $P=4\ \text{nW}$, respectively. The optical characteristics for the $500\ \text{nm}$ ($R_0=40\ \Omega$) and $250\ \text{nm}$ ($R_0=6.79\ \Omega$) devices are also similar to each other but, remarkably, opposite to those of the 5 and $1\ \mu\text{m}$ devices as can be seen in Fig. 2(b). Here the resistance *increases* drastically with increased illumination. The different physical process now prevalent must overcome the reduction in the resistance originating from nonequilibrium carriers.

Carriers traversing the semiconductor exhibit diffusive transport with resistivity $\rho=1/(n\mu e)$, determined by the concentration (n) and mobility (μ). The product $n\mu$ increases upon illumination;¹⁰ thus, above band-gap illumination of 5 and $1\ \mu\text{m}$ devices reduces their four-point resistance as do the carriers traveling through the shunt. Given the opacity of the shunt, the observed response can be clearly distinguished from the lateral photovoltaic effect.¹¹ These negative photoresistive results are similar to the photo response of a macroscopic In/GaAs MSH structure with an Ohmic sidewall interface that has recently been reported.¹² In both cases the photo response is amplified by the geometry of the device and the current pathway provided by a metal shunt.

A comparative study of dynamic responses for different size devices with respect to light intensity is presented in Fig. 4. The response curves clearly demonstrate a wide dynamic range, as high as 40 dB, for our nanoscale devices. By considering the Gaussian beam profile, the opaque shunt and contacts, and the absorbance of the illuminated region of the doped GaAs epilayer we find $\delta R(P)$ values for the $500\ \text{nm}$ and $250\ \text{nm}$ devices of 965% ($1.0\ \text{nW}$) and 9462% ($0.25\ \text{nW}$), respectively. The optical characteristics of the $500\ \text{nm}$ control device are similar to that of the 5 and $1\ \mu\text{m}$ devices but the maximum $\delta R(P)$ is only 6% ($2\ \text{nW}$). With a maximum power density of $1\ \text{W}/\text{cm}^2$ of $632.8\ \text{nm}$ radiation and radiative recombination¹³ the steady state photoinduced carrier density is $n_{ph} \approx 1.5 \times 10^{16}\ \text{cm}^{-3}$.¹⁴ This alone accounts well for the 6% $\delta R(P)$ of the control device and emphasizes the enhancement of $\delta R(P)$ by the shunt.

To interpret our results, we note that if the lateral geometry and placement of the shunt and leads is preserved, the measured $R(P)$ values should depend only on the steady state resistivity. If the same recombination process is prevalent in each device, n_{ph} is fixed and the devices would have approximately equal resistances at maximum illumination. As can be seen from Fig. 4, the values of $R(P)$ for all four devices are within a factor of 2 under maximum illumination and we conclude that all devices are diffusive in this limit. The photoresponse in the submicron devices can be explained by considering quasiballistic carrier transport in addition to the diffusive transport.¹⁵ When the relevant length scales of the conductor become comparable to the momentum mean free path of the carriers, λ_p , electrons can travel ballistically.^{6,16} Here, the resistance is determined by the contact resistance and is sensitive to interactions with the boundaries.¹⁷

Transport measurements of the GaAs epitaxial layer of our devices⁷ have determined that $18 \text{ nm} \leq \lambda_p \leq 35 \text{ nm}$ for $2 \text{ K} \leq T \leq 300 \text{ K}$. Because of the space constriction for the submicron devices and fabrication limitations the actual separation of the Ohmic leads and shunt (L) varies from 20 to 40 nm for the 500 nm device and 15 to 30 nm for the 250 nm device. Hence for these devices $L \sim \lambda_p$ and $L < \lambda_p$, respectively. Thus, in the dark, the majority of the carriers travel ballistically across the gap between injector contact and shunt. This accounts for the (counter intuitive) small value of R_0 for the nanoscopic devices. The larger $\delta R(P)$ values of the 250 nm device relative to the 500 nm device can also be attributed to the ballistic and quasiballistic traversal of the carriers. For smaller separation between the lead and shunt a larger proportion of electrons travel ballistically; hence the response to illumination will be more acute for smaller gap devices. Presumably, the increase in $\delta R(P)$ with decreasing device size will ultimately be limited by boundary scattering.

Our explanation for the observed SDPP is summarized as follows: At low bias, the introduction of a sufficient density of photoinduced carriers gives rise to additional scattering (from photoionized traps or scattering centers) resulting in a transition from ballistic to diffusive transport and a corresponding increase in resistance.¹⁸ If this increase in resistance is greater than the reduction due to the photoinduced carrier density (6%) and the influence of the shunt, a positive photoresistance will result. The exact mechanism for the conversion from ballistic to diffusive transport will depend on the specifics of the excitation and recombination mechanisms; however, the lower R_0 of the 500 and 250 nm devices supports the assertion that these are in the ballistic regime and the convergence of the resistance of all four devices within a factor of 2 under maximal illumination supports a size-independent final diffusive state.

To evaluate the sensitivity of SDPP sensors using a conventional figure of merit we have calculated the specific detectivity, $D^* = R_V \sqrt{A_D} / V_n$ at minimum illumination, where $R_V = \Delta V / \Delta P$ is the responsivity, A_D is the active area of detection, V_n is the root-mean-square noise voltage per unit bandwidth, ΔP is the incident power on the active area, and ΔV is the corresponding voltage change.¹⁹ For the 250 nm

device, we find a resistance change of 16.7Ω for $2.5 \times 10^{-14} \text{ W}$ laser power after passing through a 40 dB ND filter. Since, the current through the device was 100 nA, $R_V = 6.68 \times 10^6 \text{ V/W}$. In the Johnson noise limit, V_n can be replaced by the thermal noise voltage, $V_n = (4kTR_0)^{1/2}$ where k is Boltzmann's constant.²⁰ For the 250 nm device, $D^* = 5.06 \times 10^{11} \text{ cm} \sqrt{\text{Hz/W}}$. This is competitive with the published D^* values of much larger individually addressable photodetectors.^{21,22} [The D^* values for the 5 μm , 1 μm , and 500 nm devices were 2.0, 1.0, and $3.3 \times 10^{11} \text{ cm} \sqrt{\text{Hz/W}}$, respectively.]

This work is supported by the U.S. NIH (Grant No. 1U54CA11934201), the U.S. NSF (Grant No. ECCS-0725538), and the UK EPSRC (Grant No. EP/F065922). W.J.C. was partially supported from the ERC for Advanced Bioseparation Technology, KOSEF, Korea. S.A.S. and S.A.W. are cofounders of and have a financial interest in PixelEXX, Inc., a start-up company whose mission is to market imaging arrays. K.D.W. and A.K.M.N. also have a financial interest in PixelEXX.

¹A. Vaseashta and D Dimova-Malinovska, *Sci. Technol. Adv. Mater.* **6**, 312 (2005).

²K. Fife, A. E. Gamal, and H.-S. P. Wong, *Tech. Dig. - Int. Electron Devices Meet.* **2007**, 986.

³M. Law, D. J. Sirbuly, J. C. Johnson, J. Goldberger, R. J. Saykally, and P. Yang, *Science* **305**, 1269 (2004).

⁴M. J. Chou, D. C. Tsui, and G. Weimann, *Appl. Phys. Lett.* **47**, 609 (1985).

⁵H. Nakanishi, K. J. M. Bishop, B. Kowalczyk, A. Nitzan, E. A. Weiss, K. V. Tretyakov, M. M. Apodaca, R. Klajn, J. F. Stoddart, and B. A. Grzybowski, *Nature (London)* **460**, 371 (2009).

⁶M. Heiblum, M. I. Nathan, D. C. Thomas, and C. M. Knoedler, *Phys. Rev. Lett.* **55**, 2200 (1985).

⁷A. M. Gilbertson, A. K. M. Newaz, W.-J. Chang, R. Bashir, S. A. Solin, and L. F. Cohen, *Appl. Phys. Lett.* **95**, 012113 (2009).

⁸A. K. M. Newaz, Y. Wang, J. Wu, S. A. Solin, V. R. Kavasseri, N. Jin, I. S. Ahmad, and I. Adesida, *Phys. Rev. B* **79**, 195308 (2009).

⁹S. M. Sze, *Physics of Semiconductor Devices*, 2nd ed. (Wiley-Interscience, New York, 1981), pp. 793–795.

¹⁰D. L. Rode and S. Knight, *Phys. Rev. B* **3**, 2534 (1971).

¹¹J. T. Wallmark, *Proc. IRE* **45**, 474 (1957).

¹²K. A. Wieland, Y. Wang, L. R. Ram-Mohan, S. A. Solin, and A. M. Girgis, *Appl. Phys. Lett.* **88**, 052105 (2006).

¹³U. Strauss, W. W. Ruhle, and K. Kohler, *Appl. Phys. Lett.* **62**, 55 (1993).

¹⁴See supplementary material at <http://dx.doi.org/10.1063/1.3480611> for a derivation of the photoinduced carrier density.

¹⁵R. de Picciotto, H. L. Stormer, L. N. Pfeiffer, K. W. Baldwin, and K. W. West, *Nature (London)* **411**, 51 (2001).

¹⁶J. R. Hayes, A. F. Levi, and W. Wiegman, *Phys. Rev. Lett.* **54**, 1570 (1985).

¹⁷S. Datta, in *Electronic Transport in Mesoscopic Systems*, edited by H. Ahmed, M. Pepper, and A. Broers (Cambridge University Press, Cambridge, 1995).

¹⁸R. Lipperheide, T. Weis, and U. Wille, *J. Phys.: Condens. Matter* **13**, 3347 (2001).

¹⁹M. Shaban, K. Nomoto, S. Izumi, and T. Yoshitake, *Appl. Phys. Lett.* **94**, 222113 (2009).

²⁰A. Van Der Ziel, *Noise in Solid State Devices and Circuits* (Wiley, New York, 1986).

²¹G. N. Lu, J. M. Galvan, C. Jeloyan, G. Goumy, and V. Marcoux, *Mater. Sci. Eng., C* **C21**, 203 (2002).

²²K. H. Lee, R. W. Chuang, P. C. Chang, S. J. Chang, Y. C. Wang, C. L. Yu, J. C. Lin, and S. L. Wu, *J. Electrochem. Soc.* **155**, H959 (2008).